

Supplementary material

Silvia Innocenti¹, Alain Mailhot¹, and Anne Frigon²

¹Centre Eau-Terre-Environnement, INRS, 490 de la Couronne, Québec, Canada, G1K 9A9

²Consortium Ouranos, 550 Sherbrooke Ouest, Montréal, Canada, H3A 1B9

Correspondence to: S. Innocenti (silvia.innocenti@ete.inrs.ca)

Introduction

This supporting information presents some extended results and describes in more details in some methodological developments. It is structured as follows. Figure S1 displays the station locations and the median of precipitation intensity AMS for some durations considered in the study. Figures S2 and S3 show results for the SS model validation (Slope and GOF tests)

5 when AMS are separated according to the tip and temporal resolution. Section S1 briefly describe these figures. Figure S4 presents the regional distribution of the mean wet time, \bar{T}_{wet} , of the events sampled within each 6-duration scaling interval, while the detailed definition of \bar{T}_{wet} is given in Sect. S2. Finally, Fig. S7 to S15, extend to longer scaling intervals the analysis presented in Sect. 4.3 (Regional analysis) and Sect. 5.2 (SS-GEV model evaluation) for 6-duration scaling intervals.

Section S1: Details on Fig. S2 and S3 .

Figures S2 and S3 show the results of the Slope and GOF tests applied at the 0.05 significance level when AMS are separated according to the tip and temporal resolution of the recording station. Each of the 12 matrix of these figures represents the proportion of valid SS stations [see the definition of valid SS station in Sect. 4.1 and in Fig. 1 (e) of the paper] for each duration 5 (vertical axis) and scaling intervals (horizontal axis). Each grid-box of the heatmaps is divided in two triangles.

Upper triangles in Fig. S2 correspond to the fraction of AMS having tip resolution $< 2.54 \text{ mm}$, while lower triangles correspond to AMS with tip resolution of 2.54 mm . Tip resolution at each station is defined as the minimum non-zero recorded value. Tip resolution at stations having both DM and H series, or both 15PD and HPD series, was defined as the maximum value between the resolutions of these two series.

- 10 Upper triangles in Fig. S3 correspond to the fraction of AMS constructed from both HPD and 15PD series, or both H and MD series (i.e. with temporal resolution $\leq 1 \text{ h}$). Lower triangles correspond to the fraction of AMS constructed from hourly series only (series constructed from HPD or H series, i.e. a 1h temporal resolution).

White triangles in Fig. S2 and S3 indicate non-significant differences between upper and lower triangle proportions. Tests on proportion differences were applied at significance level 0.05 without accounting for the spatial autocorrelation among stations.

Section S2: Definition of the Mean Wet Time, \bar{T}_{wet} , of the Events Sampled Within Each Scaling Interval.

For each station, the mean wet time, \bar{T}_{wet} [hours], of events sampled within each scaling interval was computed as:

$$\bar{T}_{wet} = n_E^{-1} \sum_e^{n_E} T_{wet,e} \quad (\text{S1})$$

with n_E the total number of events e sampled by the annual maxima precipitation series in the scaling interval [see Sect. 4.3

5 of the article for the definition of each event]. $T_{wet,e}$ is the wet time of the e^{th} event:

$$T_{wet,e} = W_e T_e \quad (\text{S2})$$

where W_e is the fraction of event time steps during which positive precipitation depths were recorded, and T_e is the total event duration (in hours).

Figure S4 displays the distribution over valid SS stations of \bar{T}_{wet} within each region [Fig. S4 (a) to (f)] and one example of

10 calculation of $T_{wet,e}$ and \bar{T}_{wet} [Fig. S4 (g)].

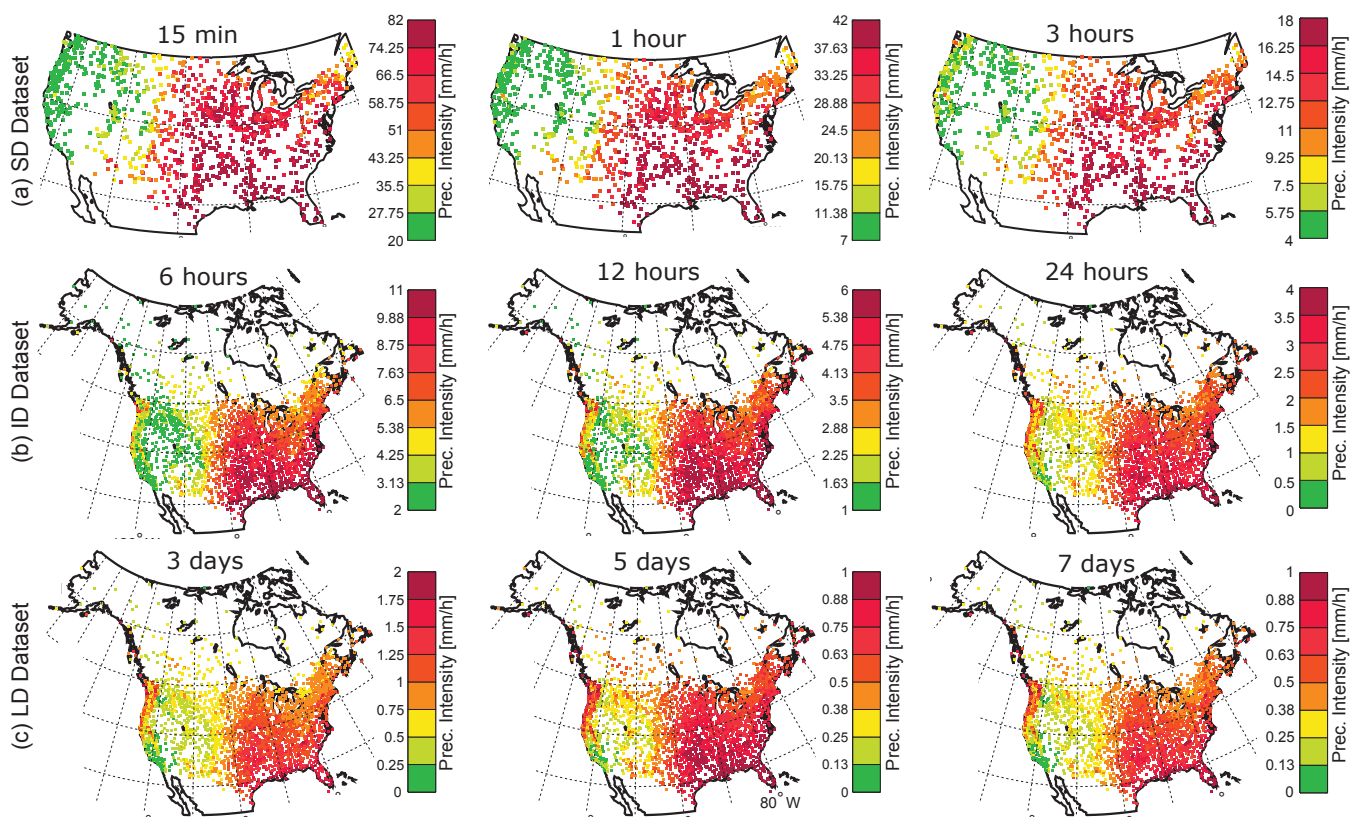


Figure S1. Spatial distribution of the median precipitation intensity for: (a) 15 min, 1 h, and 3 h in the SD dataset, (b) 6 h, 12 h, and 24 h in the ID dataset, and (c) 3days, 5days, and 7days in the LD datasets.

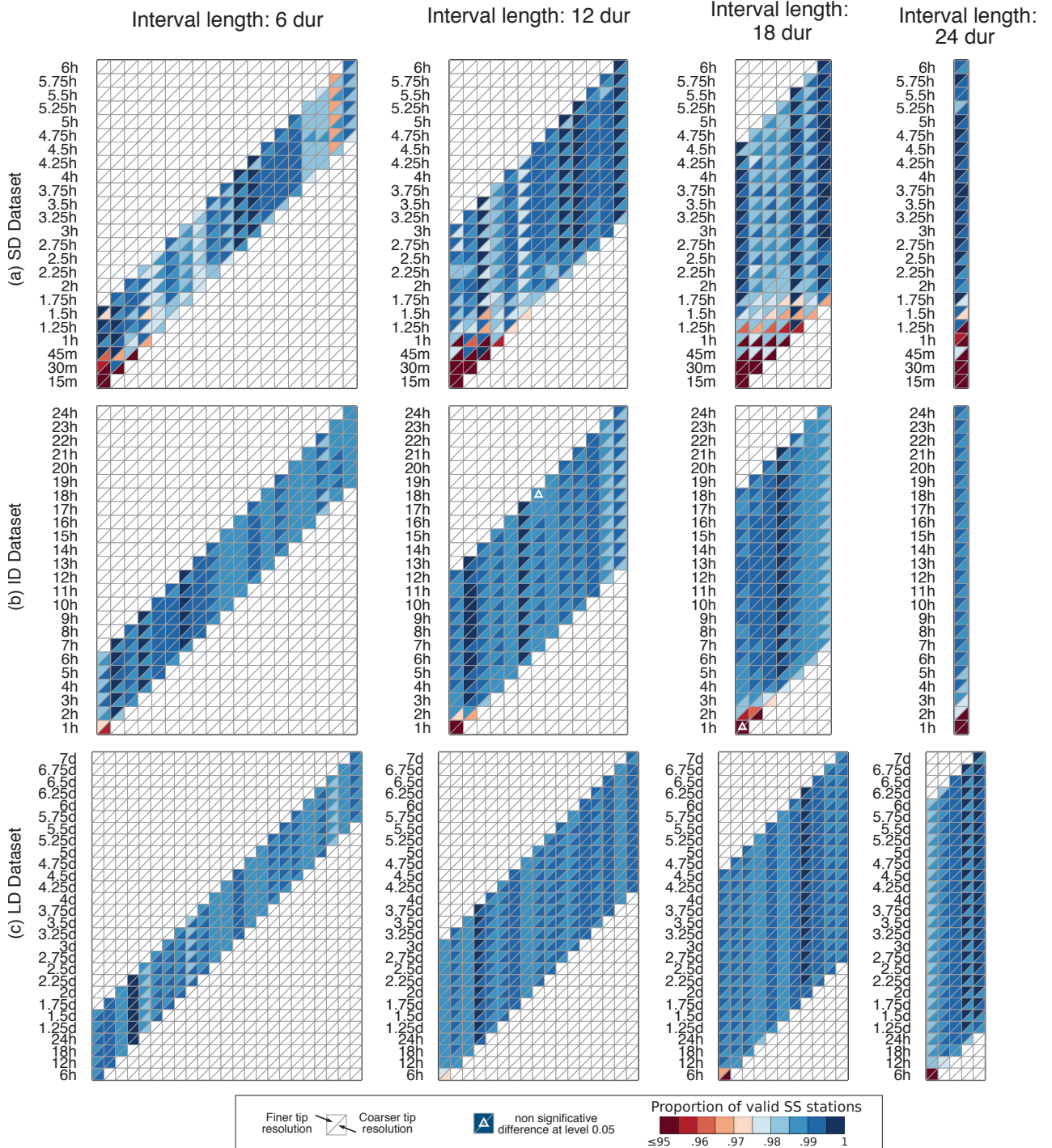


Figure S2. Proportion of valid SS stations for each duration and scaling interval for the SD, ID, and LD datasets [row (a), (b), and (c) respectively] when accounting for series tip resolutions. Upper triangles correspond to the fraction of AMS having tip resolution < 2.54 mm, while lower triangles correspond to AMS with tip resolution of 2.54 mm. White triangles indicate non-significant differences between upper and lower triangle proportions. See Section S1 for details.

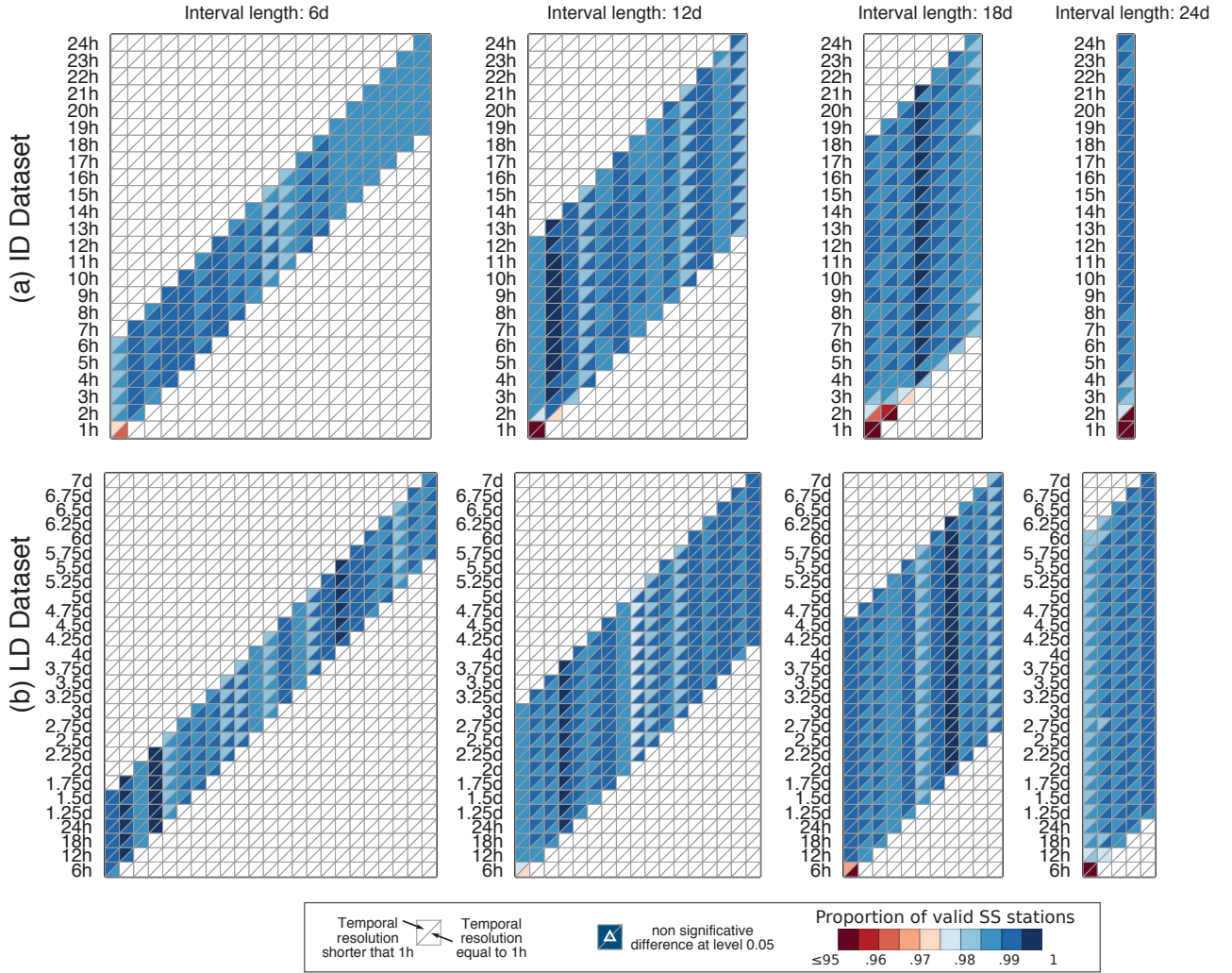


Figure S3. Proportion of valid SS stations for each duration and scaling interval for (a) ID and (b) LD datasets when accounting for series temporal resolutions. Upper triangles in Figures S3 correspond to the fraction of AMS with temporal resolution ≤ 1 h. Lower triangles correspond to the fraction of AMS constructed from hourly series only. White triangles indicate non-significant differences between upper and lower triangle proportions. See Section S1 for details.

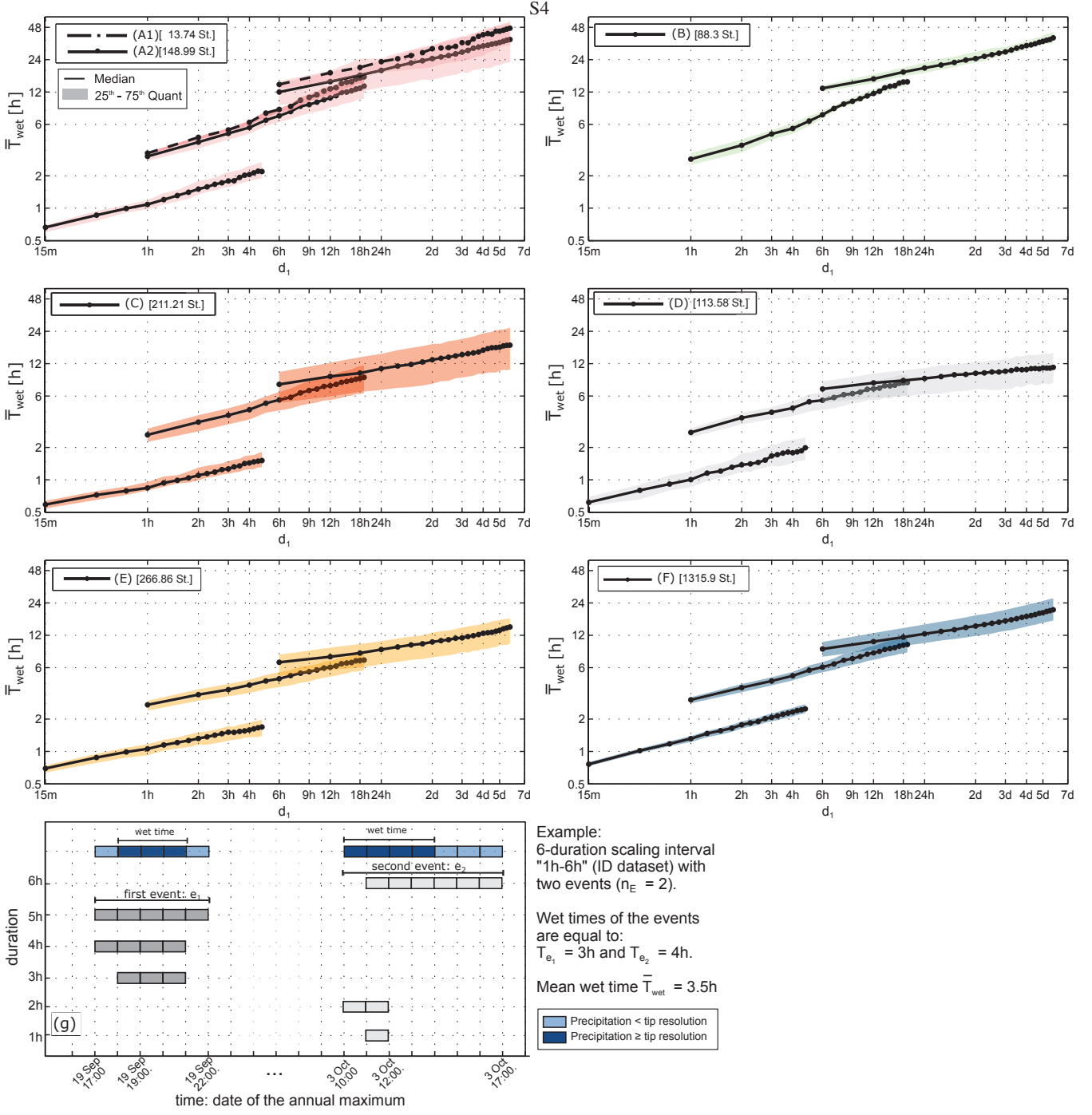


Figure S4. Median and Interquantile Range (IR) of the distribution over valid SS stations of the mean wet time, \bar{T}_{wet} , within each region for each 6-duration scaling interval in the SD (left curve), ID (central curve), and LD (right curve) datasets. Graph (g) displays an example of how \bar{T}_{wet} is estimated for one theoretical scaling interval. For each region, the mean number of valid SS stations over the scaling intervals is indicated in brackets.

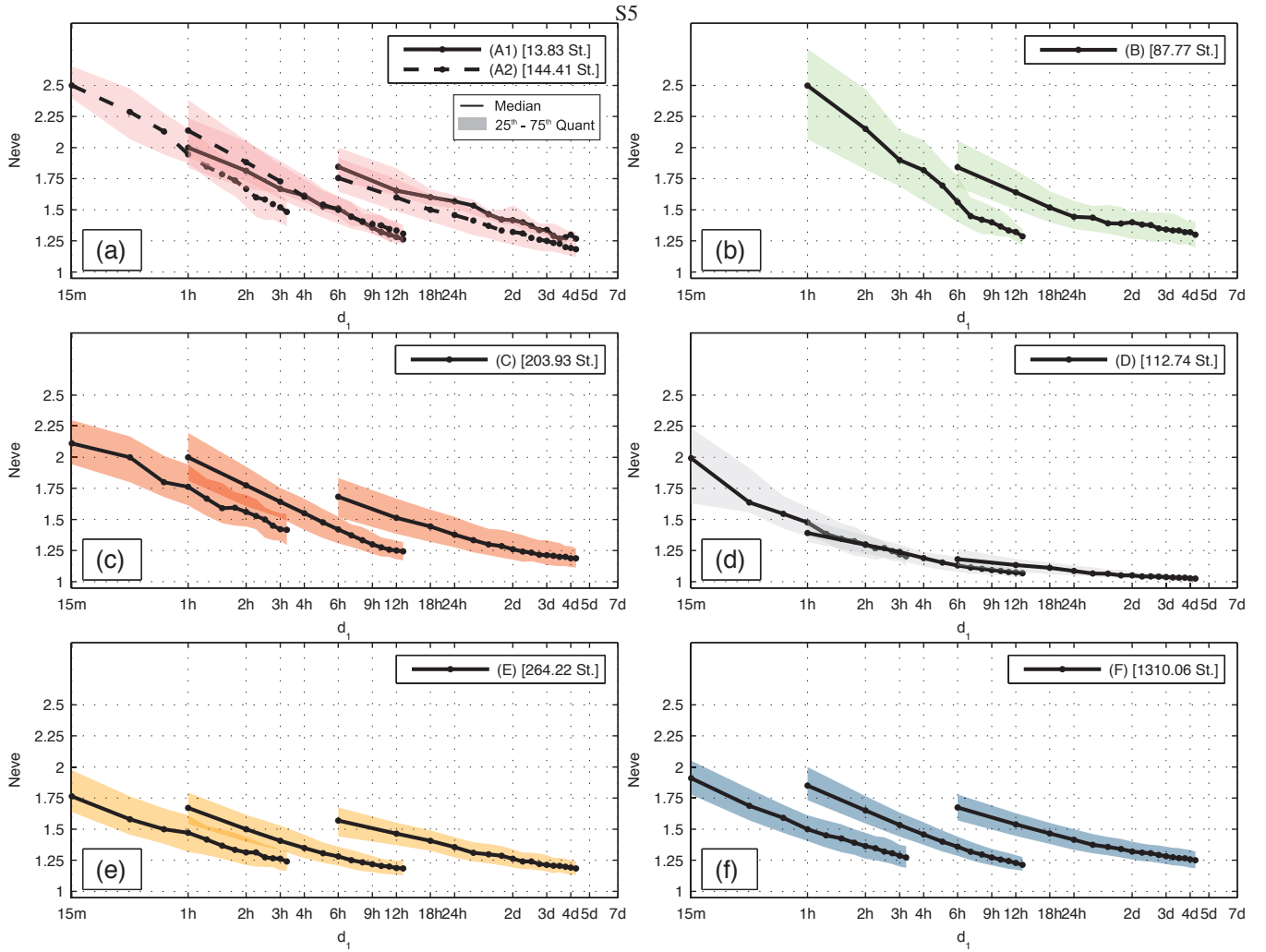


Figure S5. Median and Interquartile Range (IR) of the distribution over valid SS stations of the mean number of events per year, \bar{N}_{eve} , within each region for each 12-duration scaling interval for the SD (left curve), ID (central curve), and LD (right curve) datasets. For each region, the mean number of valid SS stations over the scaling intervals is indicated in brackets.

S6

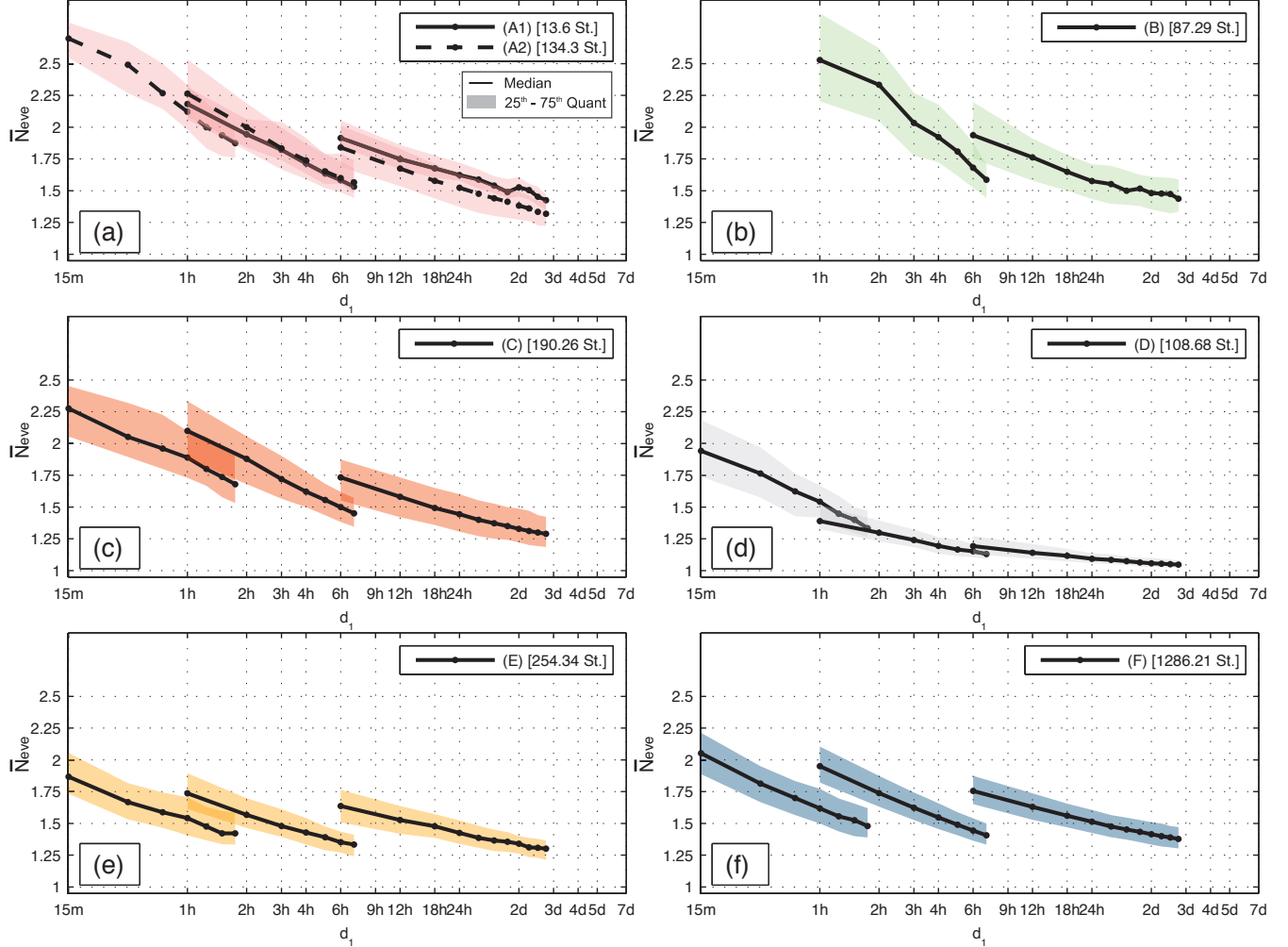


Figure S6. Median and Interquantile Range (IR) of the distribution over valid SS stations of the mean number of events per year, \bar{N}_{eve} , within each region for each 18-duration scaling interval for the SD (left curve), ID (central curve), and LD (right curve) datasets. For each region, the mean number of valid SS stations over the scaling intervals is indicated in brackets.

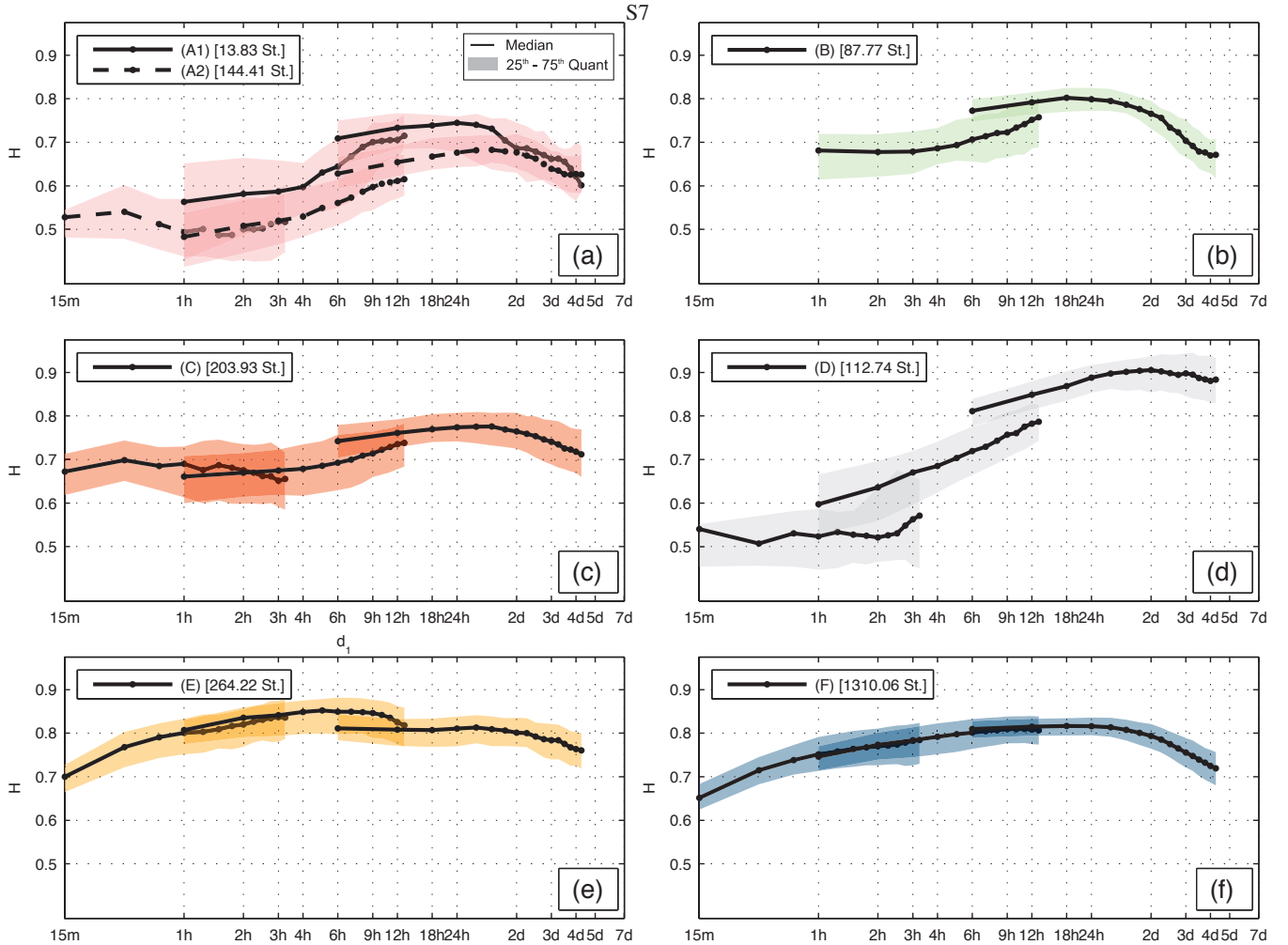


Figure S7. Median and Interquartile Range (IR) of the scaling exponent distribution over valid SS stations within each region for 12-duration scaling intervals in the SD (left curve), ID (central curve), and LD (right curve) datasets. For each region, the mean number of valid SS stations over the scaling intervals is indicated in brackets.

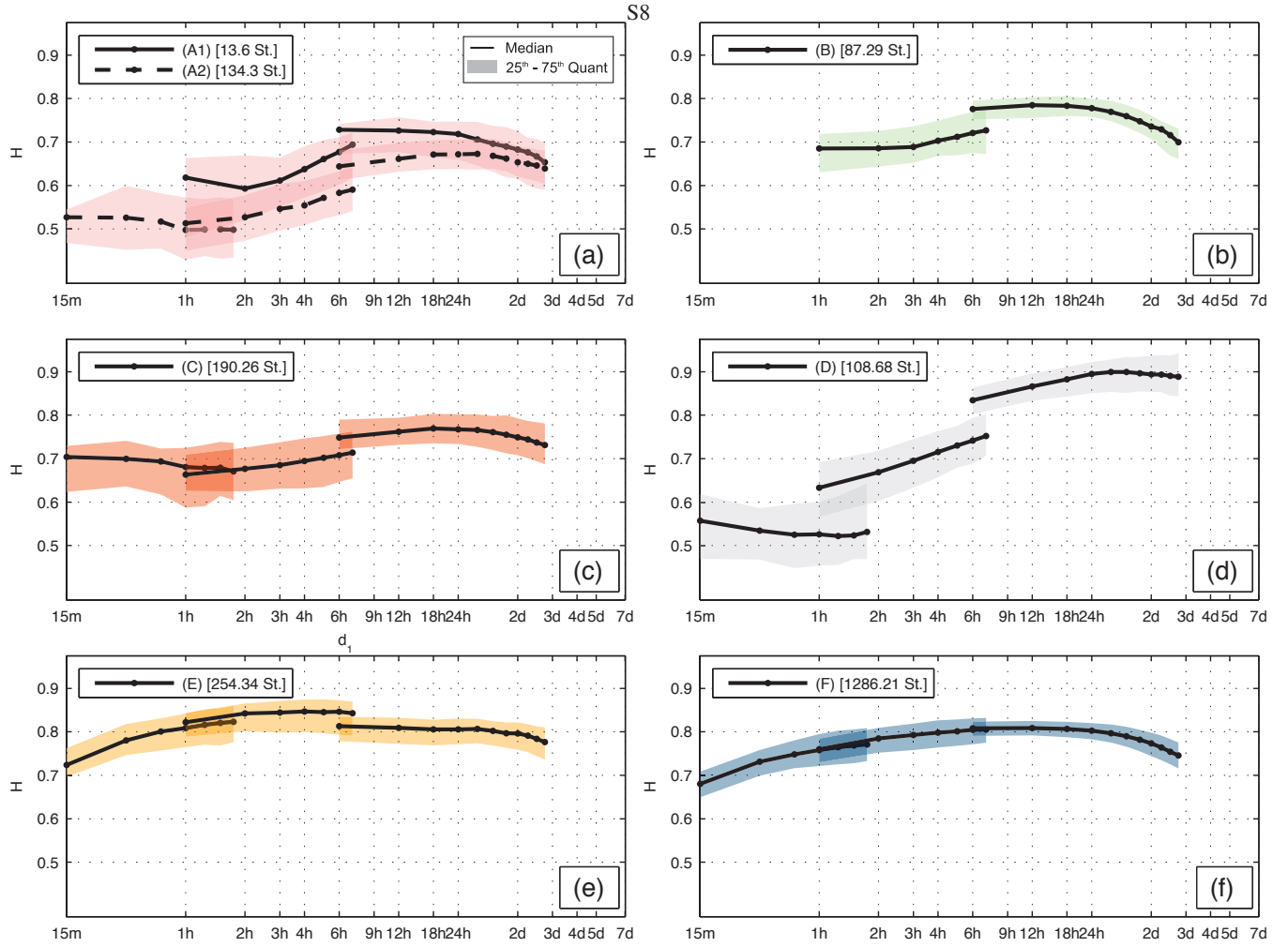


Figure S8. Median and Interquartile Range (IR) of the scaling exponent distribution over valid SS stations within each region for 18-duration scaling intervals for the SD (left curve), ID (central curve), and LD (right curve) datasets. For each region, the mean number of valid SS stations over the scaling intervals is indicated in brackets.

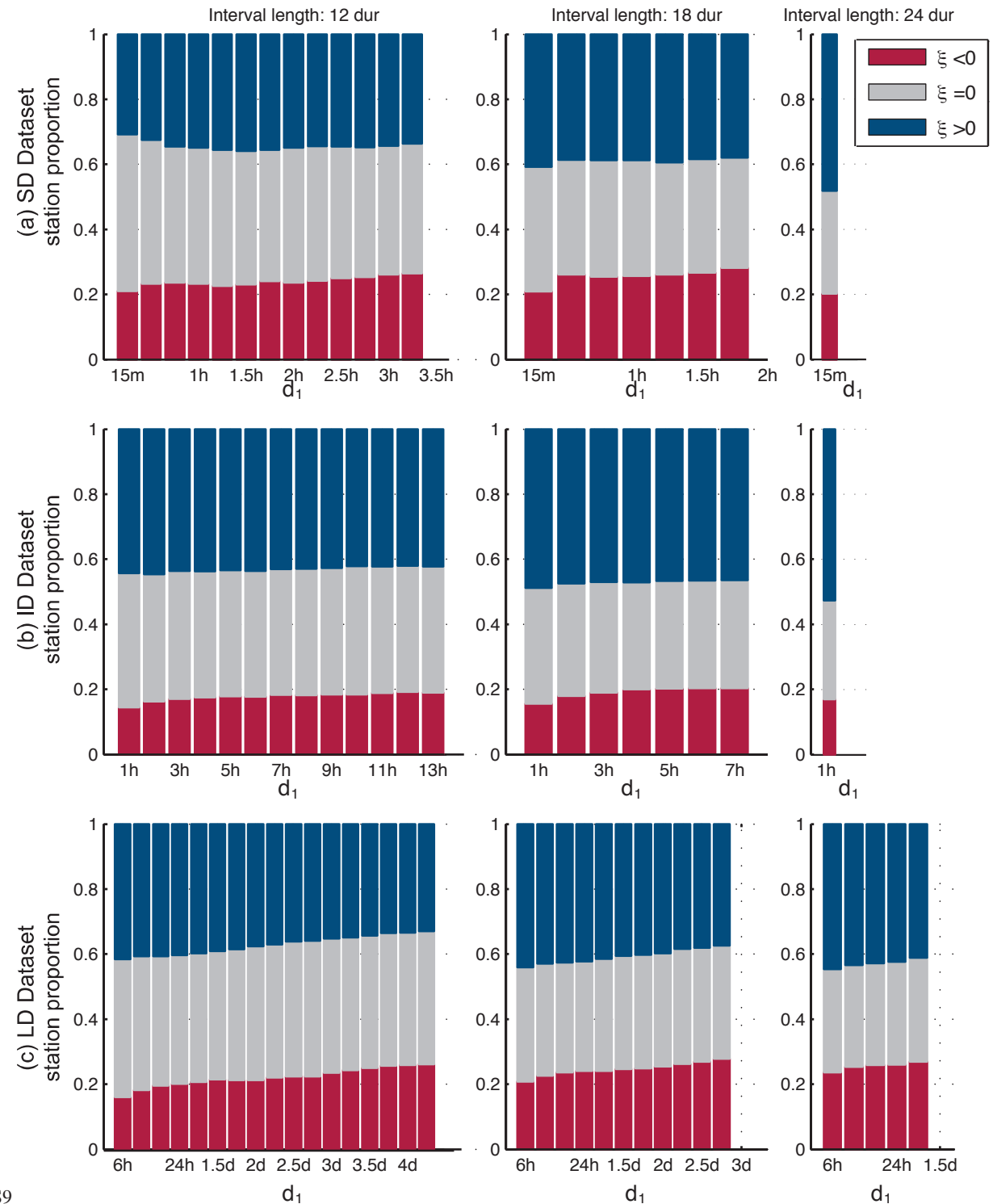


Figure S9. Stacked proportion of valid SS stations with $\xi < 0$ (in red), $\xi = 0$ (in grey), and $\xi > 0$ (in blue) for each 12-, 18-, and 24-duration scaling interval [1^{st} , 2^{nd} , and 3^{rd} col., respectively] in SD, ID, and LD datasets [(a), (b), and (c), respectively].

S10

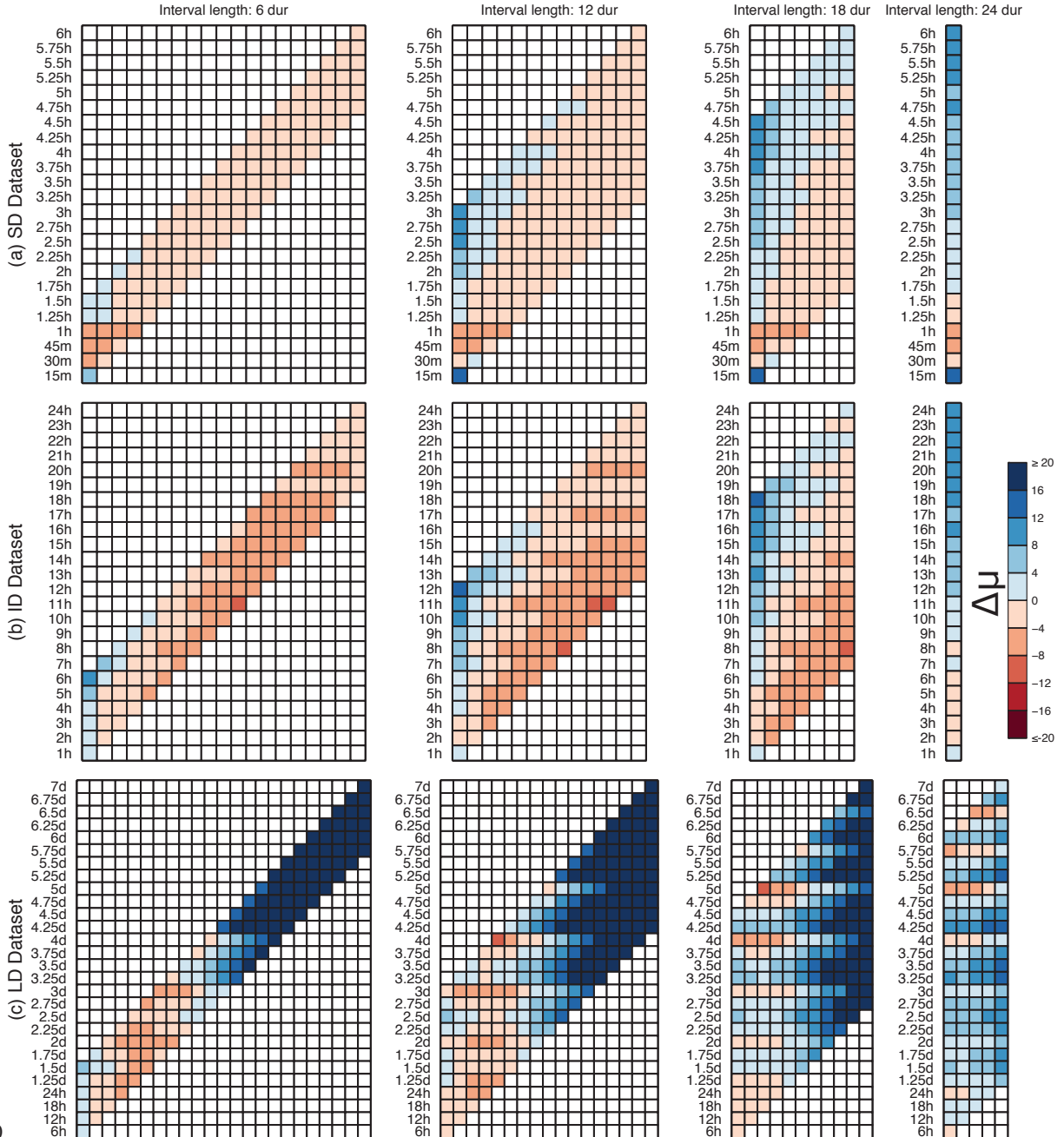


Figure S10. Median Δ_μ for each for each scaling interval (horizontal axis) and duration (vertical axis) in SD, ID, and LD datasets [(a), (b), and (c), respectively] .

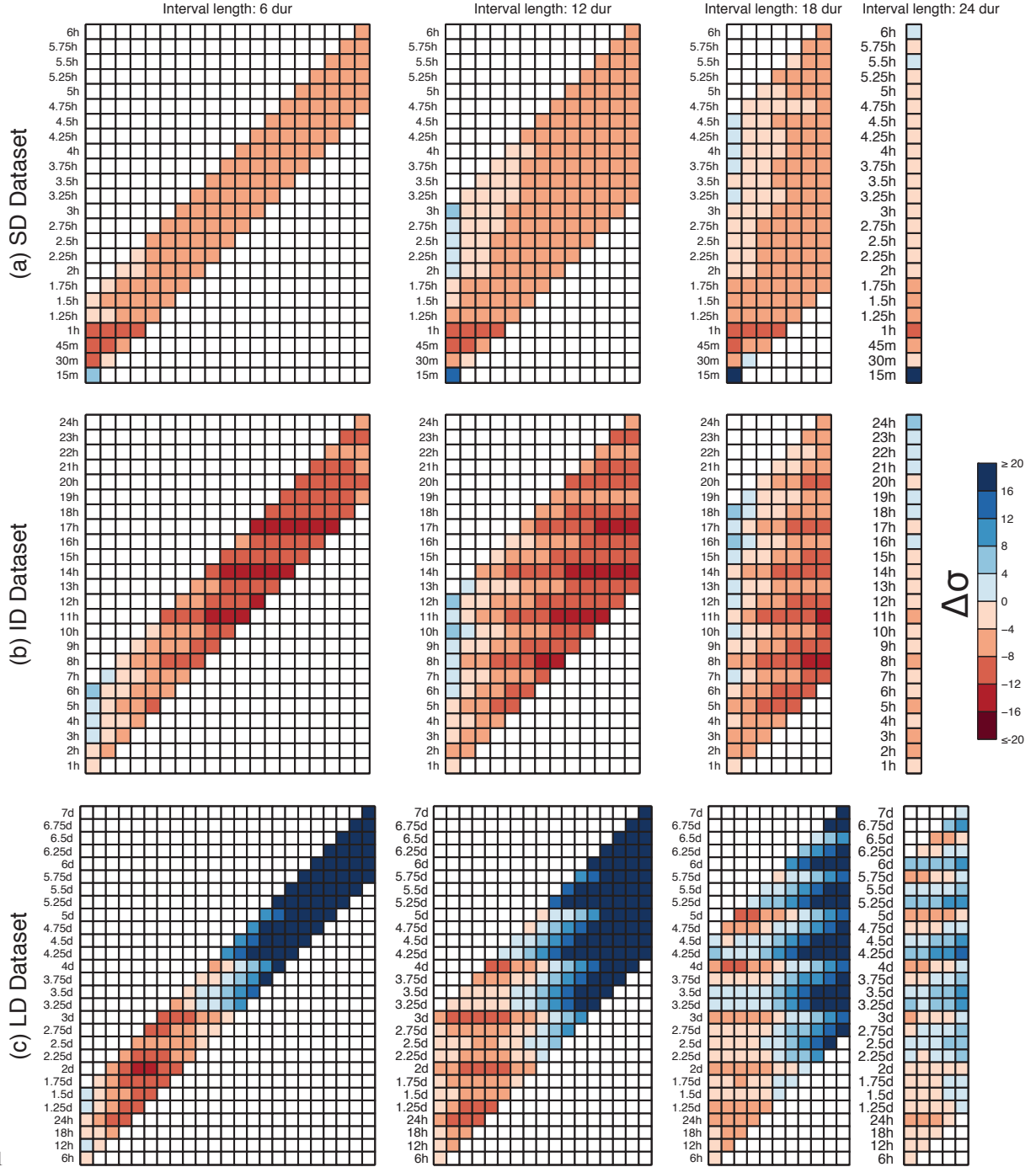
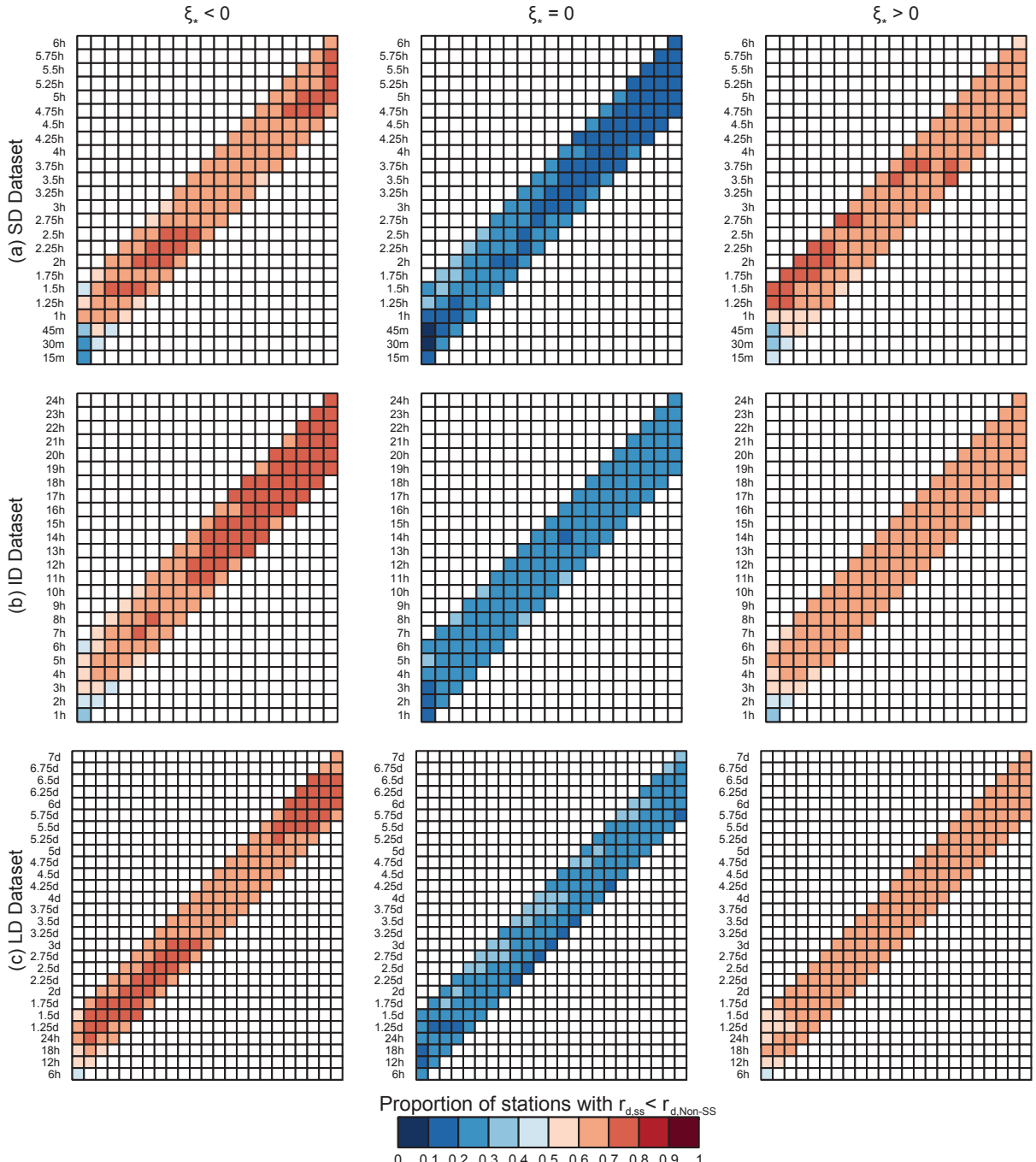


Figure S11. Median Δ_σ for each scaling interval (horizontal axis) and duration (vertical axis) in SD, ID, and LD datasets [(a), (b), and (c), respectively].



S12

Figure S12. Proportion of valid SS stations having $r_{d,ss} < r_{d,non-SS}$ for $\xi_* < 0$ (1^st col.), $\xi_* = 0$ (2^{nd} col.), and $\xi_* > 0$ (3^{rd} col.) for each 6-duration scaling interval (horizontal axis) and duration (vertical axis) in SD, ID, and LD datasets [(a), (b), and (c), respectively].

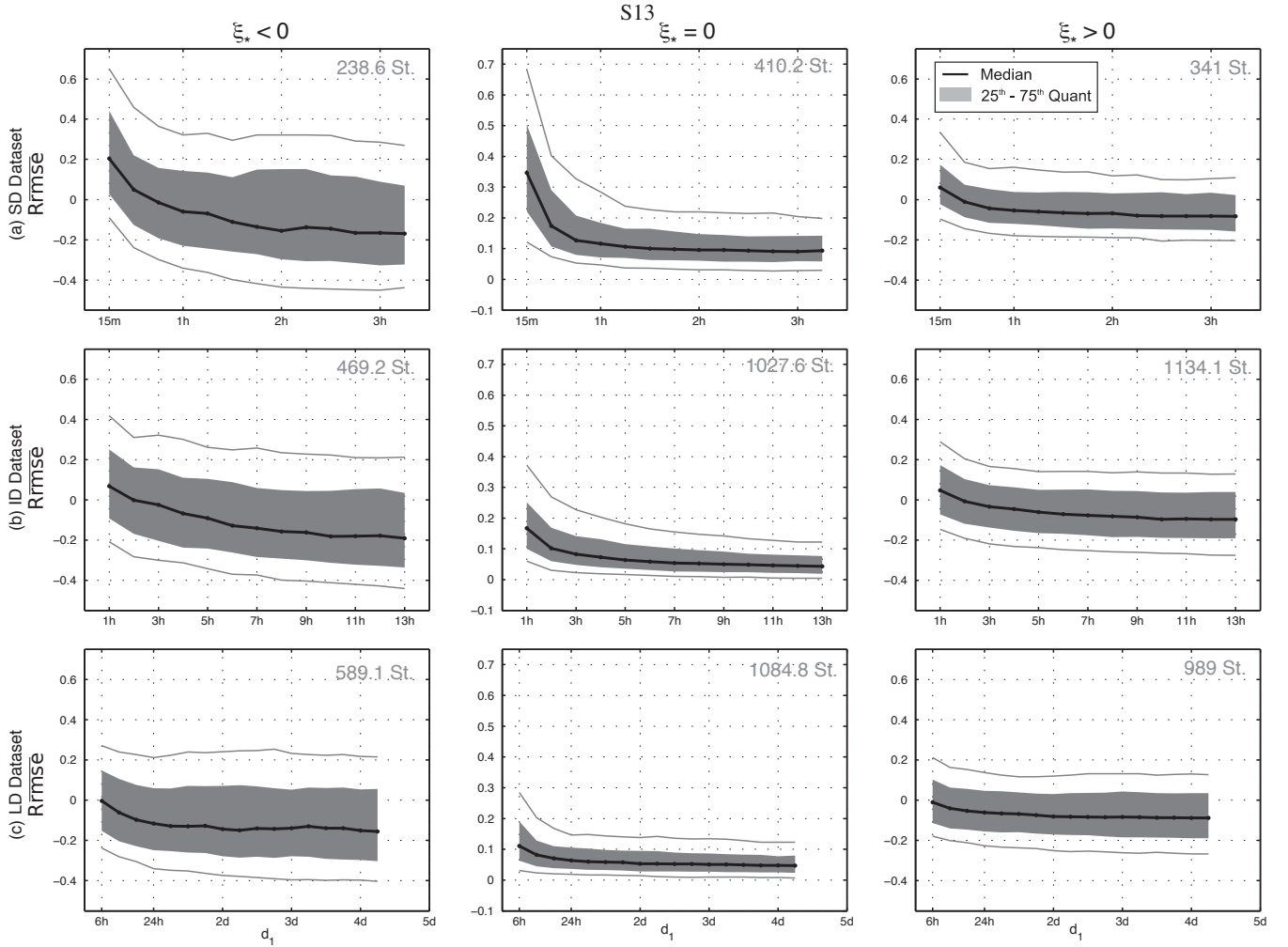


Figure S13. Distribution of the relative total RMSE ratio, R_{RMSE} , for $\xi_* < 0$ (1st col.), $\xi_* = 0$ (2nd col.), and $\xi_* > 0$ (3rd col.) for 12-duration scaling intervals in SD, ID, and LD datasets [(a), (b), and (c), respectively].

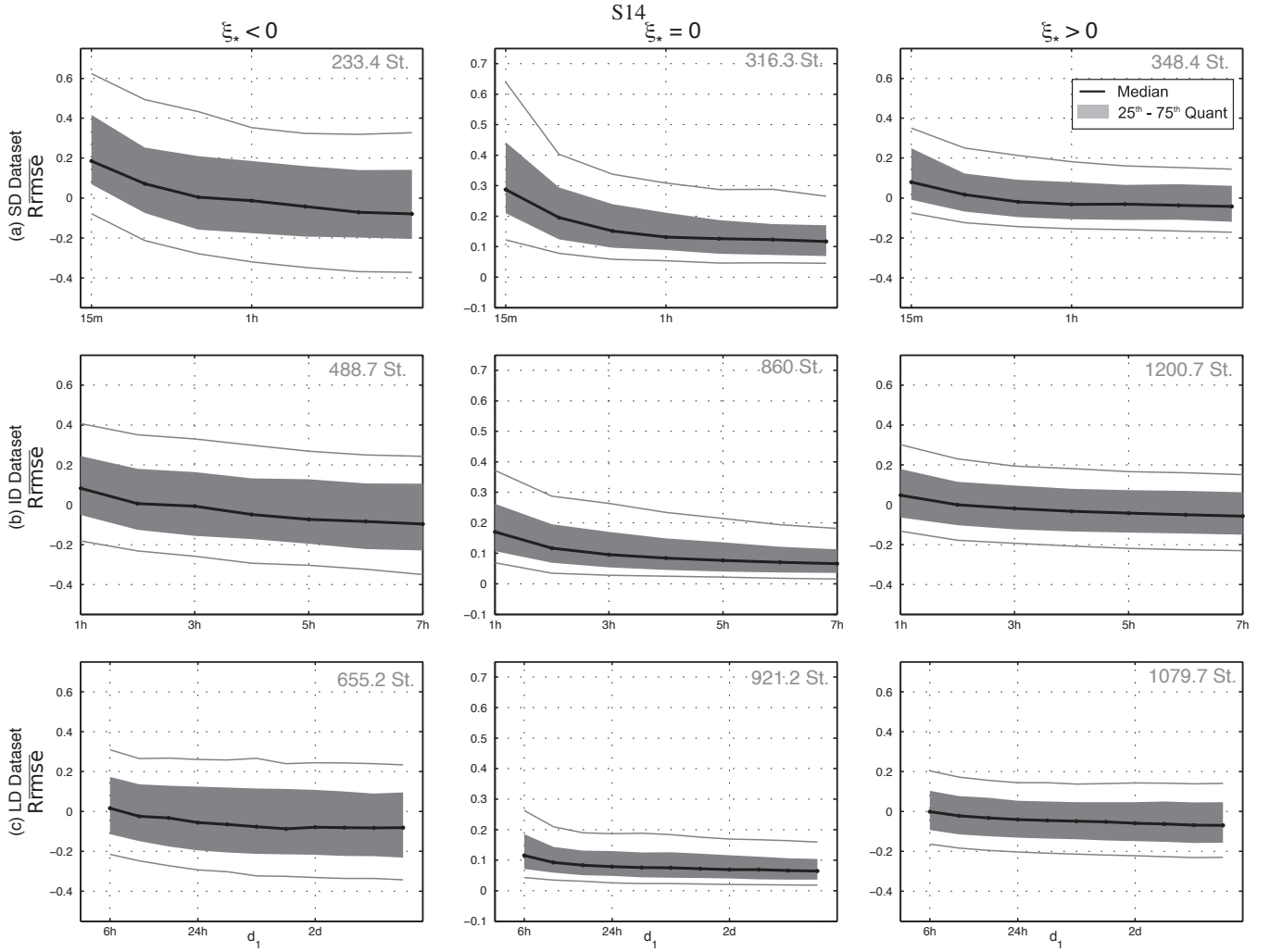


Figure S14. Distribution of the relative total RMSE ratio, R_{rmse} , for $\xi_* < 0$ (1st col.), $\xi_* = 0$ (2nd col.), and $\xi_* > 0$ (3rd col.) for 18-duration scaling intervals in SD, ID, and LD datasets [(a), (b), and (c), respectively].

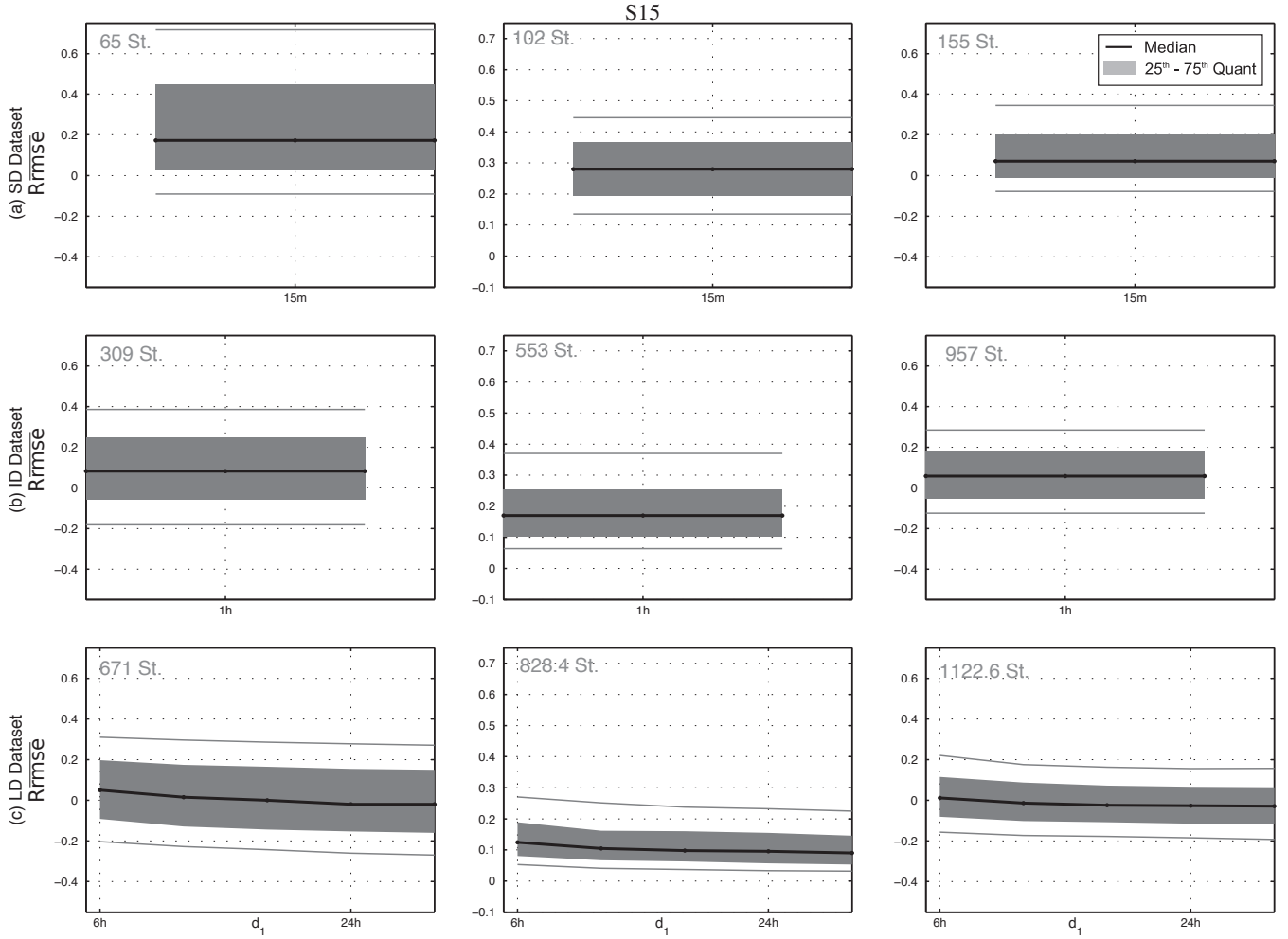


Figure S15. Distribution of the relative total RMSE ratio, R_{rmse} , for $\xi_* < 0$ (1st col.), $\xi_* = 0$ (2nd col.), and $\xi_* > 0$ (3rd col.) for 24 duration scaling intervals in SD, ID, and LD datasets [(a), (b), and (c), respectively].